

Effect of Li doping on magnetic and transport properties of CoV_2O_4 and FeV_2O_4

Prashant Shahi¹, R. Singh¹, Shiv Kumar², D. K. Dubey^{1,3}, D. N. Singh^{1,3}, A. Tiwari⁴, A. Tripathi⁴,
A. K. Ghosh² and Sandip Chatterjee^{1,*}

¹Department of Physics, Indian Institute of Technology (Banaras Hindu University), Varanasi-221 005, India

²Department of Physics, Banaras Hindu University, Varanasi-221 005, India

³Department of Physics, National Institute of Technology Durgapur, India

⁴Department of Physical Sciences, School of Chemical and Physical Sciences, Sikkim University, Sikkim, India

Abstract

The structural, magnetic and transport properties have been studied of Li doped CoV_2O_4 and FeV_2O_4 . Li doping increases the ferri-magnetic ordering temperature of both the samples but decreases the spin-glass transition temperature of CoV_2O_4 . The Li-doping decreases the V-V distance which in effect increases the A-V coupling. Thus the increased A-V coupling dominates over the decrease in A-V coupling due to doping of non-magnetic Li.

*Corresponding author *e-mail id:* schatterji.app@iitbhu.ac.in

Ph.No. & Fax No.: +91-5426701913

Introduction

Transition- metal- oxide (TMO) spinels is becoming the centre of attraction with significant quality of complex interaction among charge, spin and orbital degrees of freedom which gives it some interesting properties. Importantly, vanadium spinel oxides AV_2O_4 ($A = Fe^{2+}, Mn^{2+}, Co^{2+}, Zn^{2+}, Mg^{2+}$), where A^{2+} and V^{3+} ions occupy the tetrahedral (A site) and octahedral (B site) sites, respectively, have two 3d electrons in the triply degenerate t_{2g} states at V^{3+} site. This whole arrangement is becoming the centre of attention and also their fascinating magnetic and orbital order [1–7]. When A site is replaced by some non magnetic ion [Li, Zn, Mg, Cd] it shows many interesting properties. Likewise ZnV_2O_4 goes from cubic to tetragonal state at $T=50$ K and orders antiferromagnetically at $T= 42$ K [8] and LiV_2O_4 shows metallic behavior and it is a first transition metal oxide which shows heavy fermion behavior and remains in cubic phase in its whole temperature range [9-11]. On the other hand, when A site is replaced by Magnetic ions, different properties emerges. In this way the MnV_2O_4 exempts magnetic phase transition from the collinear ferrimagnetic order to the non-collinear canted one at 53 K with associations to the anti-ferro-orbital order of vanadium t_{2g} orbitals [3, 12]. Whereas, CoV_2O_4 exhibits two magnetic phase transitions at 142 K and 59 K without any structural phase transitions [13, 14].

Moreover, FeV_2O_4 is a unique compound among such spinel vanadium oxides comprising both Fe^{2+} and V^{3+} ions with orbital degrees of freedom; Fe^{2+} ion at the tetrahedral site (A-site) having three 3d electrons in the doubly degenerate e_g states. Very recent development shows structural and magnetic properties of the spinel FeV_2O_4 [11] exhibiting successive structural transitions from cubic to compressed tetragonal with the lattice constants of $c < a$ at $T_{s1} \sim 140$ K which is due to the cooperative Jahn–Teller effect of FeO_4 and from tetragonal to orthorhombic transition accompanied by a ferrimagnetic transition at $T_{s2} \sim 110$ K, and from orthorhombic to elongated tetragonal with $c > a$ at $T_{s3} \sim 60$ K with decreasing temperature for polycrystalline samples. It has also been reported that the Jahn–Teller effects and the relativistic spin–orbital coupling play an important role in the determination of the orbital states of Fe^{2+} and V^{3+} ions at low temperatures which were concluded with the help of single crystal x ray diffraction experiments [6]. Recent reports of NMR and neutron diffraction of FeV_2O_4 indicate that its structure is changing to non-collinear ferrimagnetic state at 60 K from collinear state, where the V^{3+} moments become mounted along the $\{111\}$ directions [7, 15]. This latter transition is marked

by a step in magnetization, a peak in heat capacity, an anomaly in the dielectric constant, and the appearance of polarization. It was found that the application of a magnetic field shifts all these signatures associated to T_{s3} to higher temperatures, while it also clearly affects the value of the polarization, revealing a significant magneto electric coupling. It is suggested that the presence of canted spins in the triangular structure below T_{s3} could be responsible for the appearance of ferroelectricity [16].

The AV_2O_4 system also approaches the itinerant-electron limit with decreasing V-V separation [17,18]. The predicted critical separation for metallic behavior is $R_c = 2.94 \text{ \AA}$ [19]. A recent study on FeV_2O_4 and CoV_2O_4 shows that with increasing pressure the V-V separation decreases and due to which there is a delocalization of charge carriers in FeV_2O_4 and it induces metallic behavior in CoV_2O_4 [14]. The same effect is also shown by chemical pressure by doping Co at the site of MnV_2O_4 [20]. Recently it is shown that in FeV_2O_4 , CoV_2O_4 and MnV_2O_4 the magnetic transition temperature suppressed and activation energy decreases as Zn^{2+} (non magnetic ion) increases at the A site [21-23]. Furthermore, Li^{1+} is also a non magnetic ion and its size is comparable to Mn, Zn, Fe and Co but Li^{1+} has no 3d electron in their outer shell unlike Fe and Co. Therefore, it will be interesting to investigate the magnetic and transport properties by doping Li in CoV_2O_4 and FeV_2O_4 at the A site.

Furthermore, soft magnetic materials are center to nearly every aspect of modern electrical and electronics technology because of their ability to concentrate and to shape magnetic flux with great efficiency. The most important Characteristics desired for essentially all soft magnetic applications are high saturation induction, high permeability, low coercivity, and low core loss .So these Materials are also good subject for these application.

In this paper, we have investigated magnetic and transport properties of $Li_xCo_{1-x}V_2O_4$ ($0 \leq x \leq 0.2$) and $Li_xFe_{1-x}V_2O_4$ ($0 \leq x \leq 0.1$) and found that with increasing the Li content at Co and Fe site the Ferrimagnetic transition temperature increases for bothe the systems, the spin glass magnetic transition is suppressed in CoV_2O_4 and the systems are moving towards iterant electron limit due to decrease in the V-V distance.

Experiment

The polycrystalline $\text{Li}_x\text{Co}_{1-x}\text{V}_2\text{O}_4$ ($0 \leq x \leq 0.2$) and $\text{Li}_x\text{Fe}_{1-x}\text{V}_2\text{O}_4$ ($0 \leq x \leq 0.1$) samples used in this study were prepared by solid state reaction method. Appropriate ratio of Li_3VO_4 , Fe, Fe_2O_3 , CoO, V_2O_3 and V_2O_5 were grounded thoroughly and pressed into pellets. The pellets were sealed in evacuated quartz tube and heated at 1050°C for 40 hours for $\text{Li}_x\text{Fe}_{1-x}\text{V}_2\text{O}_4$ ($0 \leq x \leq 0.1$) and at 900°C for $\text{Li}_x\text{Co}_{1-x}\text{V}_2\text{O}_4$ ($0 \leq x \leq 0.2$). The X-ray powder diffraction experiment has been performed using Rigaku Mini Flex II DEXTOP X-ray Diffractometer with Cu- α radiation. Magnetic measurement was done using MPMS SQUID (Quantum Design) magnetometer with the bulk samples. Ac-susceptibility measurement were done using lock in amplifier SRS830 by homemade setup and standardized with YBCO superconducting sample. Fourier Transform Infrared Spectroscopy measurements have been done using Spectrum 65 FTIR spectrometer (Perkin Elmer Instruments, USA) in the range of 500 to 4000 cm^{-1} . Resistivity measurements have been done via four probe method.

Result and Discussion

Figure 1 shows the X-ray diffraction (XRD) pattern for different Li doped samples. All peaks are indexed as Fd-3m space group indicating our samples are of pure phase. Inset of the figure 1 shows variation of lattice parameter with Li Doping, obtained from the Rietveld refinement of the XRD data. It is observed that with increasing the Li concentration at the Fe and Co site the lattice parameters decrease linearly following the Vegard's law. The ionic size of Li is 0.73\AA which is comparable to Co (0.72\AA) and smaller than Fe (0.77\AA). But in both the cases lattice parameters are decreasing which might be due to the fact that Co have seven 3d electrons and Fe have six 3d electrons due to which there is strong coulomb repulsion between Co/Fe and oxygen 2p electrons but due to lithium doping the coulomb repulsion decreases as it has no 2p and 3d electrons in its outer shell. The parameters obtained from Reitveld refinement are given in the Table 1. Figure 2 and figure 3 show the variation of magnetization with temperature for $\text{Li}_x\text{Co}_{1-x}\text{V}_2\text{O}_4$ ($0 \leq x \leq 0.2$) and $\text{Li}_x\text{Fe}_{1-x}\text{V}_2\text{O}_4$ ($0 \leq x \leq 1$) which shows that as we are increasing the Li content at Co and Fe site the ferrimagnetic transition temperature also increasing but the second magnetic transition is suppressed by Li doping in CoV_2O_4 . We have also measured ac-susceptibility at 100 Hz for $\text{Li}_x\text{Co}_{1-x}\text{V}_2\text{O}_4$ ($0 \leq x \leq 2$) and $\text{Li}_x\text{Fe}_{1-x}\text{V}_2\text{O}_4$ ($0 \leq x \leq 1$) which is shown in

figure 4 and figure 5 respectively. Similar behavior is observed for both the cases that with increasing Li content at A site the ferrimagnetic transition temperatures increase. This might be due to the fact that shrinkage of the lattice parameter with Li doping, increases the exchange interaction between the A^{2+} and V^{3+} through oxygen which enhances the ferrimagnetic ordering temperature. On the other hand, the saturated moment, which is estimated from the isothermal magnetization curve (shown in Figure 6), decreases monotonously upon Li doping. Since Li ions are non-magnetic, it is known that V spins tend to align anti-parallel to each other when the coupling between A and B sub-lattices is absent. Therefore the moment of the V sub-lattice also decreases with increasing Li content. As a result it decreases monotonously. It is important to compare these with the earlier studies on $Zn_xMn_{1-x}V_2O_4$ [23] and $Co_{1-x}Zn_xV_2O_4$ [22] because Zn(0.74Å) is also a non magnetic ion. Moreover, the sizes of Li (0.73Å), Co (0.72Å) and Zn (0.74Å) are comparable. In case of $Zn_xMn_{1-x}V_2O_4$ it is found that as the Zn content increases the magnetic transition temperature decreases which is different than that in Li doped samples. With Zn doping two cases arises, the lattice parameters decrease with increasing Zn content due to which the V-V distance decreases so that coupling between A and V sites increase which tries to increase the magnetic transition temperature. But doping of non magnetic ion at A site decreases the A-V coupling due to which V-V spins try to align anti-parallel. As a result, the magnetic transition is suppressed [23]. The same case also arises in case of $Co_{1-x}Zn_xV_2O_4$ [22]. The second effect is more dominant in case of Zn doping but in our case the first effect is dominating due to which the magnetic transition temperature increases with Li doping. Similar behavior is observed in $Mn_{1-x}Co_xV_2O_4$ system where with increasing magnetic Co content the ferrimagnetic transition temperature increases along with the decrease of V-V distances [20]. In the present systems it might be the case that non-magnetic Li doping converts some V^{3+} into V^{4+} which might be the reason of increasing the A-V coupling. From Figure 2 we have found that the spin glass behavior, which is present in case of CoV_2O_4 at 59 K is also suppressed with Li^{1+} doping. This may be due to the weakening of magnetism at the Co^{2+} sub-lattice due to doping of non magnetic Li^{1+} which may weaken the coupling between Co^{2+} and V^{3+} sub-lattice and due to which the spin glass behavior is suppressed with Li doping. Opposite behavior is observed when non-magnetic Zn is doped in $Cd_{1-x}Zn_xV_2O_4$ system [24]. Zn doping increases the V-V distance which in effect induces the site disorder. Figure 7 shows the variation of resistivity with temperature for all samples. As FeV_2O_4 belongs to a Mott Insulator regime and CoV_2O_4 is lying

at the itinerant electron limit therefore from inset of the figure 7 it can be mentioned that with increasing Li content at the A site the system moves towards itinerant electron side along with the decrease of V-V distance. To see the chemical pressure effect on both the systems we have plotted all our result as a function of $1/R_{V-V}$. Figure 8 shows the absorbance spectrum of $Li_xCo_{1-x}V_2O_4$ and $Li_xFe_{1-x}V_2O_4$ in the mid-infrared region. The peak observed below $\sim 1000\text{ cm}^{-1}$ corresponds to one of the four phonon modes expected for cubic spinals. The charge gap is estimated from the intersection of the linear extrapolation of the absorption edge and the frequency axis. We have also calculated the activation energy from $\ln(\rho)$ vs $1000/T$ plot and plotted the charge gap and activation energy with respect to R_{V-V} in figure 9. Both variations show the same nonmonotonic dependence of the gap as a function of chemical pressure as found in case of ZnV_2O_4 with both external and chemical pressure [25].

Conclusion

We have found that as we are increasing the Li content at A site the V-V distance decreases and due to that ferimagnetic transition temperature increases and the whole system is moving towards itinerant electron behavior. So by tuning the V-V distance either by external pressure or chemical pressure we can tune the magnetic and transport properties of AV_2O_4 samples which is very important for application point of view. Both the activation energy and charge gap show the non-monotonic dependence on chemical pressure.

Acknowledgement

SC is grateful to DST (Grant No.: SR/S2/CMP-26/2008), CSIR (Grant No.: 03(1142)/09/EMR-II) and BRNS, DAE ((Grant No.: 2013/37P/43/BRNS) for providing financial support. PS is grateful to CSIR for providing financial support.

References:

- [1] Wheeler M, Lake B, Nazmul I A T M, Reehuis M, Steffens P, Guidi T and Hill A H 2010 Phys. Rev. B 82 140406.
- [2] Lee S H et al 2004 Phys. Rev. Lett. 93 156407.

- [3] Suzuki T, Katsumura M, Taniguchi K, Arima T and Katsufuji T 2007 Phys. Rev. Lett. 98 127203.
- [4] Katsufuji T, Suzuki T, Takei H, Shingu M, Kato K, Osak K, Takata M, Sagayama H and Arima T 2008 J. Phys. Soc. Japan 77 053708.
- [5] Sakar S, Maita T, Valenti R and Saha-Dasgupta T 2009 Phys. Rev. Lett. 102 216405.
- [6] Nii Yet al 2012 Phys. Rev. B 86 125142.
- [7] MacDougall G J, Garlea V O, Aczel A A, Zhou H D and Nagler S E 2012 Phys. Rev. B 86 060414.
- [8] Ueda Y, Fujiwara N and Yasuoka H 1997 J. Phys. Soc. Jpn. 66 778.
- [9] Kondo S, Johnston D C, Swenson C A, Borsa F, Mahajan A V, Miller L L, Gu T, Goldman A I, Maple M B, Gajewski D A, Freeman E J, Dilley N R, Dickey R P, Merrin J, Kojima K, Luke G M, Uemura Y J, Chmaissem O and Jorgensen J D 1997 Phys. Rev. Lett., 78 3279.
- [10] Anderson P W 1956 Phys. Rev. 102 1008.
- [11] Johnston D C, Swenson C A and Kondo S 1999 Phys. Rev. B 59 2627.
- [13] Huang Y, Yang Z and Zhang Y, unpublished
- [14] Kismarahardja A, Brooks J S, Kiswandhi A, Matsubayashi K, Yamanaka R, Uwatoko Y, Whalen J, Siegrist T and Zhou H D 2011 Phys. Rev. Lett. 106 056602.
- [15] Katsufuji T, Suzuki T, Takei H, Shingu M, Kato K, Osaka K, Takata M, Sagayama H and Arima T 2008 J. Phys. Soc. Jpn. 77 053708.
- [16] Liu N, Zhao K H, Shi X L and Zhang L W 2012 J. App. Phys. 111 124112.
- [17] Rogers D B et al 1963 J. Phys. Chem. Solids 24 347.
- [18] Rogers D B et al 1964 J. Appl. Phys. 35 1069 .
- [19] Goodenough J B 1972 in Metallic Oxides, edited by Reiss H, Progress in Solid State Chemistry (Pergamon, New York, 1972), Vol. 5.
- [20] Kiswandhi A, Brooks J S, Lu J, Whalen J, Siegrist T and Zhou H D 2011 Phys. Rev. B 84 205138.
- [21] Ishibashi H and Kitadai Y 2012 Journal of Physics: Conference Series 391 012092.
- [22] Huang Y, Pi L, Tan S, Yang Z and Zhang Y 2012 J. Phys.: Condens. Matter 24 056001.
- [23] Shahi P, Kumar S, Sharma N, Singh R. Sastry P. U., Das A, Kumar A, Shukla K K, Ghosh A K, Nigam A K and Chatterjee S 2014 J Mater Sci 49 7317–7324.

[24]. Zhang Z, Louca D, Visinoiu A, Lee S.-H Thompson, J D, Proffen T, Llobet A, Qiu Y, Park S and Ueda Y 2006 Phys. Rev. B 74, 014108 .

[25] untscher C K, Rabia K, Forthaus M K, Abd-Elmeguid M M, Rivadulla F, Kato Y and C.D. Batista 2012 Phys. Rev. B 86 020405(R).

Table 1. Structural parameters(lattice parameters, bond engths) of $Fe_{1-x}Li_xV_2O_4$ ($0 < x < 0.1$) and $Co_{1-x}Li_xV_2O_4$ ($0 < x < 0.2$) samples obtained from Rietveld refinement of X-ray diffraction data

Sample Name	a(Å)	d(V-V)(Å ⁰)
CoV ₂ O ₄	8.4075	2.9725
Co _{0.95} Li _{0.05} V ₂ O ₄	8.3993	2.9696
Co _{0.9} Li _{0.1} V ₂ O ₄	8.3908	2.9666
Co _{0.8} Li _{0.2} V ₂ O ₄	8.3746	2.9609
FeV ₂ O ₄	8.4517	2.9881
Fe _{0.95} Li _{0.05} V ₂ O ₄	8.4429	2.9850
Fe _{0.9} Li _{0.1} V ₂ O ₄	8.4341	2.9819

Figure Captions:

1. X-ray diffraction pattern with Reitveld refinement for Li doped CoV₂O₄ and FeV₂O₄ samples at 300K. The inset shows the variation of lattice parameters with Li concentration
2. Temperature variation of magnetization for Co_{1-x}Li_xV₂O₄ [where x=0, 0.05, 0.1 and 0.2 spinels.at H=5000 Oe].
3. Temperature variation of magnetization for Fe_{1-x}Li_xV₂O₄ [where x=0, 0.05, and 0.1 spinels .at H=5000 Oe] . Inset shows the plot of dM/d T vs.T indicating transitions.

4. Temperature dependence of AC magnetization measured in fields with 100 Hz frequency for $\text{Co}_{1-x}\text{Li}_x\text{V}_2\text{O}_4$ [where $x=0, 0.05, 0.1$ and 0.2] around T_C . Inset shows the Variation of T_C with respect to $1/R_{V-V}$.
5. Temperature dependence of AC magnetization measured in fields with 100 Hz frequency for $\text{Fe}_{1-x}\text{Li}_x\text{V}_2\text{O}_4$ [where $x=0, 0.05,$ and 0.1] around T_C . Inset shows the Variation of T_C with respect to $1/R_{V-V}$.
6. The isothermal field dependence of the magnetization at 2 K for $\text{Fe}_{1-x}\text{Li}_x\text{V}_2\text{O}_4$ [where $x=0, 0.05,$ and 0.1] and $\text{Co}_{1-x}\text{Li}_x\text{V}_2\text{O}_4$ [where $x=0, 0.05, 0.1$ and 0.2], and at 80 K for $\text{Co}_{1-x}\text{Li}_x\text{V}_2\text{O}_4$ [where $x=0, 0.05, 0.1$ and 0.2] respectively.
7. The temperature dependences of resistivity for $\text{Fe}_{1-x}\text{Li}_x\text{V}_2\text{O}_4$ and $\text{Co}_{1-x}\text{Li}_x\text{V}_2\text{O}_4$.
8. Room temperature Absorbance Spectra of $\text{Co}_{1-x}\text{Li}_x\text{V}_2\text{O}_4$ [where $x=0, 0.05, 0.1$ and 0.2] and $\text{Fe}_{1-x}\text{Li}_x\text{V}_2\text{O}_4$ [where $x=0, 0.05$ and 0.1].
9. Charge gap and activation energy variation as a function of inverse V-V distance for $\text{Fe}_{1-x}\text{Li}_x\text{V}_2\text{O}_4$ [where $x=0, 0.05$ and 0.1].and $\text{Co}_{1-x}\text{Li}_x\text{V}_2\text{O}_4$ [where $x=0, 0.05, 0.1$ and 0.2].

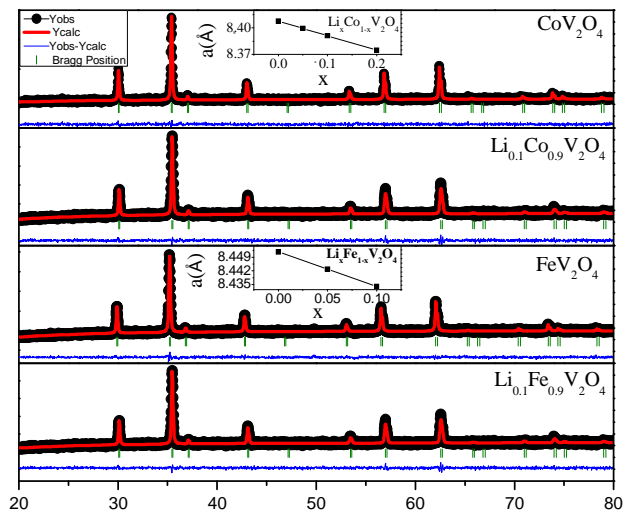


Figure 1

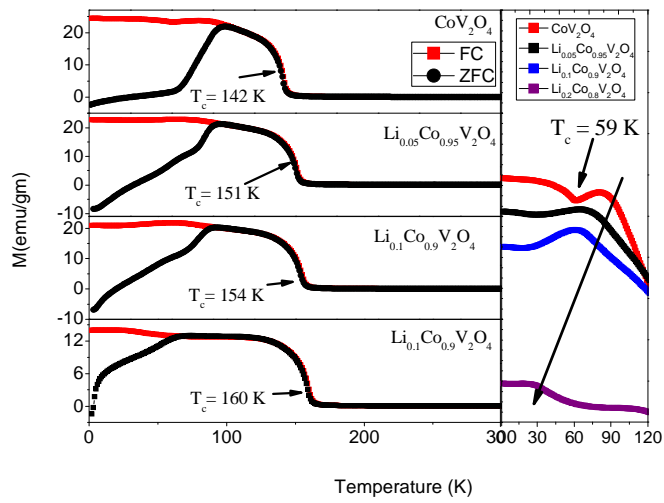


Figure 2

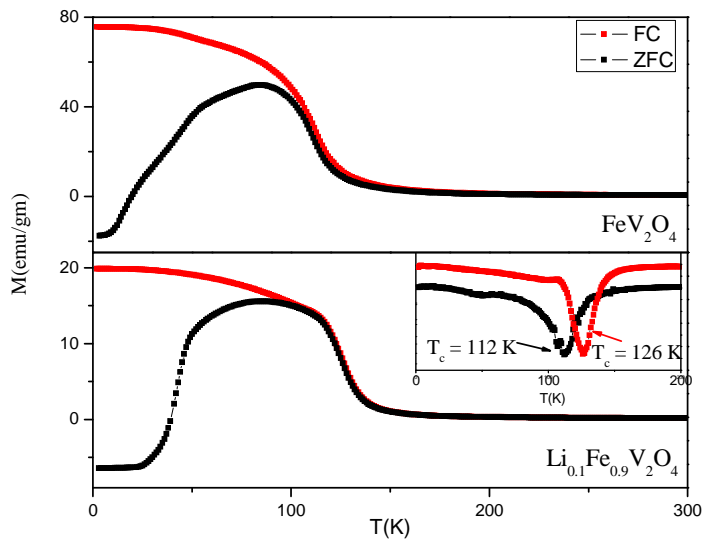


Figure 3

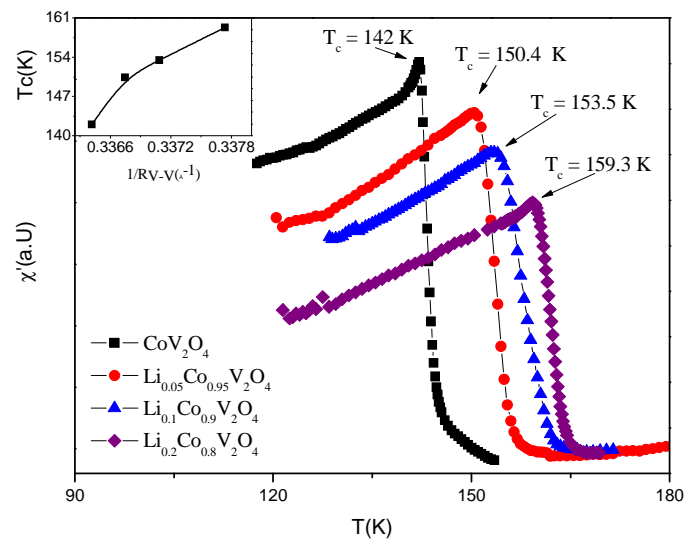


Figure 4

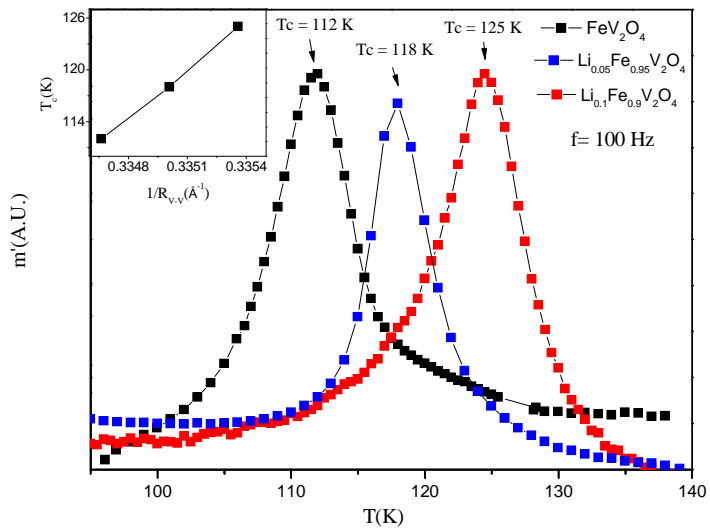


Figure 5

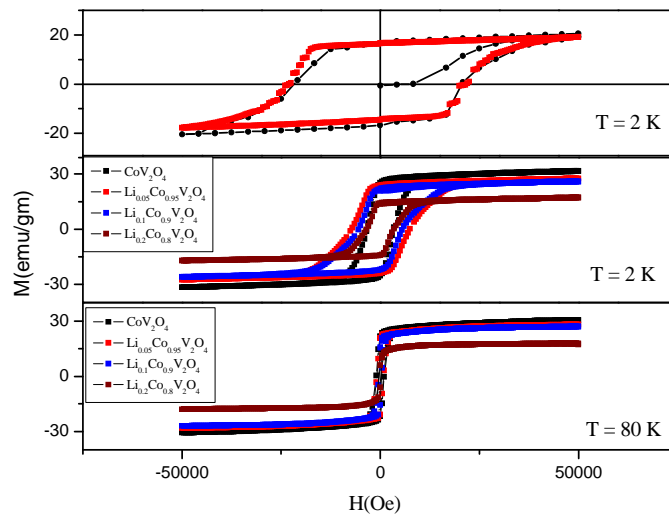


Figure 6

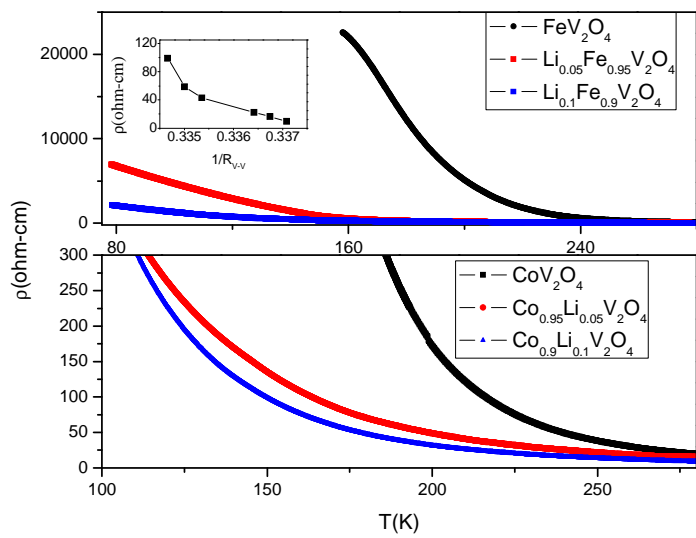


Figure 7

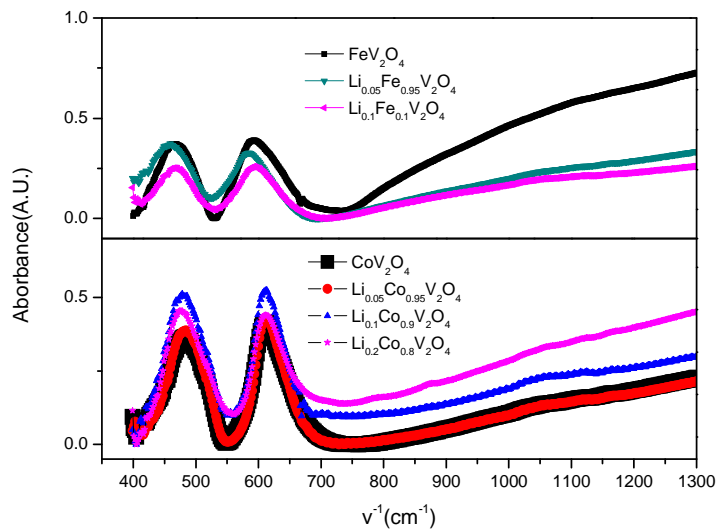


Figure 8

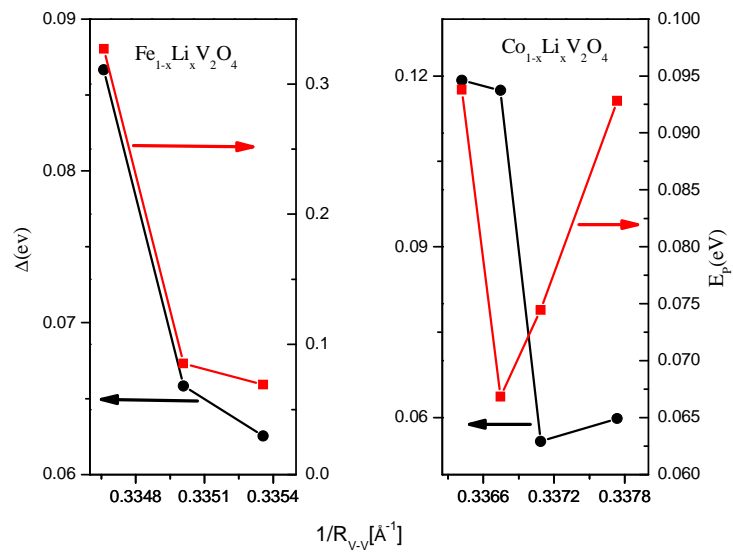


Figure 9